PROCEEDINGS OF SCIENCE

Measurement of the muon content in air showers at the Pierre Auger Observatory

Laura Collica[*a] **for the Pierre Auger Collaboration**[b]

[a] *INFN Torino, Italy*

[b] *Observatorio Pierre Auger, Av. San Martín Norte 304, 5613 Malargüe, Argentina*

E-mail: auger_spokespersons@fnal.gov

Full author list: http://www.auger.org/archive/authors_2015_06.html

The muon content of extensive air showers is an observable sensitive to the primary composition and to the hadronic interaction properties. We present here different methods which allow us to estimate the muon number at the ground level and the muon production depth by exploiting the measurement of the longitudinal, lateral and temporal distribution of particles in air showers recorded at the Pierre Auger Observatory. The results, obtained at about 10^{19} eV ($E_{\rm CM} \sim 140$ TeV center-of-mass energy for proton primaries), are compared to the predictions of LHC-tuned hadronic interaction models with different primary masses and suggest a deficit in the muon content at the ground predicted by simulations. The Pierre Auger Observatory uses water-Cherenkov detectors to measure particle densities at the ground and therefore has a good sensitivity to the muon content of air showers. Moreover, due to its hybrid design, the combination of muon measurements with other independent mass composition analyses such as $X_{\rm max}$ provides additional constraints on hadronic interaction models.

KEYWORDS: Pierre Auger Observatory, ultra-high energy cosmic rays, muons, mass composition, hadronic interactions

The 34th International Cosmic Ray Conference
30 July – 6 August, 2015
The Hague, The Netherlands

*Speaker.

PoS(ICRC2015)336

1. Introduction

The spectrum and arrival directions of Ultra High Energy Cosmic Rays (UHECRs) have been recently measured with unprecedented precision [1, 2]. However, the origin of these particles is still not well understood and remains one of the greatest priorities of the field. Establishing their composition is a crucial step to discriminate between different acceleration and propagation scenarios. Information about the composition of the primary cosmic rays has been obtained using the Fluorescence Detector (FD) of the Pierre Auger Observatory. The FD allows the measurement of the depth at which the electromagnetic component of the air shower reaches its maximum number of particles, $X_{\rm max}$ [3]. However, the interpretation of these measurements is hampered by uncertainties of the hadronic interaction models, which extrapolate interaction details from measurements in the accelerators domain to much higher energies and to different kinematic regions which are difficult to separate from the effect of the primary composition. Moreover, the FD data suffer from small statistics due to the low FD duty cycle ($\sim$15%).

The design of the Pierre Auger Observatory includes also a Surface Detector (SD) consisting of an array of water-Cherenkov detectors [4]. Different methods, which are also sensitive to primary composition, have been developed exploiting the 100% duty cycle of the SD. Among them, the study of the muon content at the ground [5] and the study of the atmospheric depth at which the muon production rate reaches a maximum in air showers [6].

Muon measurements are sensitive to the details of the hadronic component of the air shower and provide a handle to study the mass composition independently of $X_{\rm max}$. The hybrid nature of the Auger observatory provides redundancy which allows for the combination of different measurements sensitive to the primary mass to place constraints on hadronic interaction models.

2. Measurement of muon number

Recently we developed techniques to reconstruct inclined showers [7, 8] that can be used to extract the muon content of air showers. They rely on the fact that the electromagnetic component of inclined showers is largely absorbed in the atmosphere before reaching the ground. Once the shower direction is obtained using the arrival times of the SD signals, it has been shown that the number of muons per unit area at the ground level, $\rho_\mu(\theta,\phi;x,y)$, has a shape which is practically independent of energy, composition or hadronic interaction model [9, 10]. As a result it can be expressed:

$$\rho_\mu = N_{19}\,\rho_{\mu,19}(\theta,\phi;x-x_c,y-y_c), \tag{2.1}$$

where $\rho_{\mu,19}$ are the reference functions for the number densities of muons, expressed in terms of position in a plane (x,y) relative to the shower core $(x_{\rm c},y_{\rm c})$ and N_{19} is a scale factor. The reference distributions for each arrival direction are conventionally obtained from proton simulations at 10^{19} eV using the QGSJETII-03 model for hadronic interactions.

The fitted value of N_{19} gives the number of muons per unit area relative to the reference density. The total number of muons can be estimated as $N_\mu^{\rm est} = N_{19}\,N_{\mu,19}$ where $N_{\mu,19}$ is the surface integral of the $\rho_{\mu,19}$. For example, at the mean zenith angle of the data set, $\langle\theta_{\rm data}\rangle = 67^\circ$, $N_{19}=1$ would correspond to about 1.5×10^7 muons at the ground with energies above 0.3 GeV.

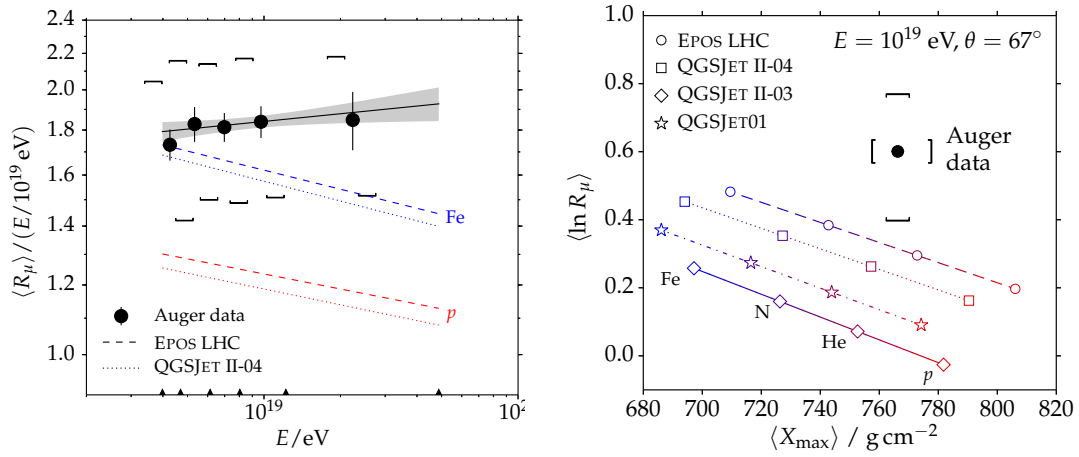

Figure 1: Left) $\langle R_\mu \rangle$ vs. primary energy, compared to air shower simulations. Right) $\langle \ln R_\mu \rangle$ vs. $\langle X_{\mathrm{max}} \rangle$. Representative primary masses are indicated by open symbols [5].

The procedure has been extensively tested with simulations comparing N_{19} to the true ratio $R_\mu^{\mathrm{MC}} = N_\mu / N_{\mu,19}$, computed as the total number of muons in the simulated shower relative to the total number of muons in the reference model. The average difference between N_{19} and R_μ^{MC} for proton or iron simulated using QGSJET01, QGSJETII-04 and EPOS-LHC is always below 5%. To get an unbiased estimator, N_{19} is corrected for the average bias of all the simulations. In the following the corrected estimator is called R_μ. By combining the uncertainty of the reference model with that of the simulated response of the SD stations to muons, we conservatively estimate the systematic uncertainty of R_μ to be 11%.

The method is applied to hybrid events with zenith angles $62° < \theta < 80°$ for which a simultaneous measurement of muon number with SD and of shower energy with FD is possible. Strict selection criteria are applied to get a high quality sample: the events must be well contained, i.e. the station closest to the fitted core and its six adjacent stations need all to be active, and only events with energy above 4×10^{18} eV are taken to ensure a 100% SD trigger probability. Quality cuts are applied for the FD to ensure an accurate reconstruction of the arrival direction and of the longitudinal profile, minimizing composition bias [11]. Out of 29722 hybrid events recorded from 1 January 2004 to 1 January 2013, 174 are accepted after quality cuts.

The relative number of muons R_μ is correlated to the shower energy by a power law

$$R_\mu = a(E/10^{19}\ \mathrm{eV})^b \tag{2.2}$$

with parameters

$$\begin{aligned} a &= \langle \ln R_\mu \rangle (10^{19}\ \mathrm{eV}) = (1.841 \pm 0.029 \pm 0.324\ (\mathrm{sys.})) \\ b &= \mathrm{d}\langle \ln R_\mu \rangle / \mathrm{d}\ \ln E = (1.029 \pm 0.024 \pm 0.03\ (\mathrm{sys.})) \end{aligned} \tag{2.3}$$

The a parameter represents the average muon content at 10^{19} eV while b is the logarithmic gain of muons with increasing energy.

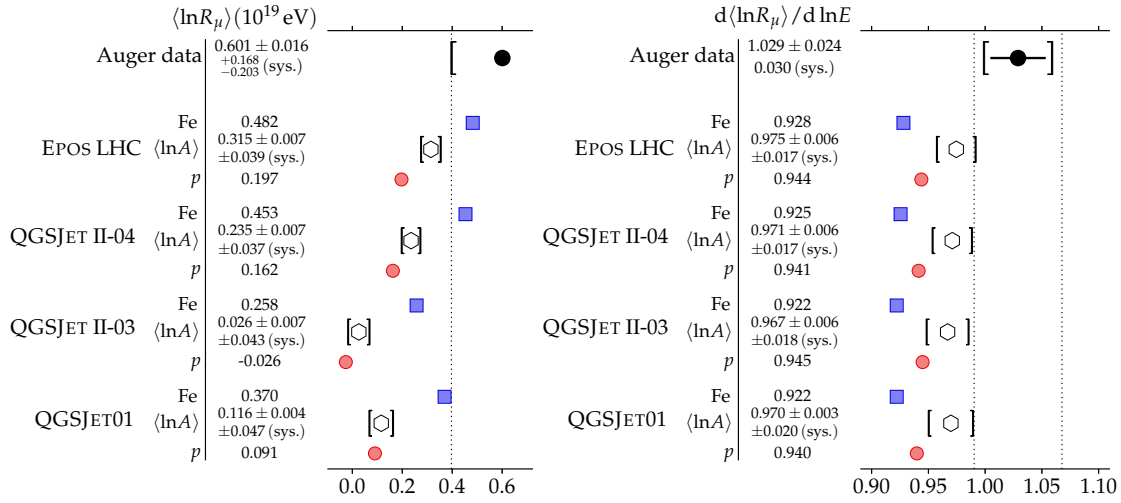

Figure 2: Comparison of $\langle \ln R_\mu \rangle$ (left) and $\mathrm{d}\langle \ln R_\mu \rangle / \mathrm{d} \ln E$ (right) between 4×10^{18} eV and 5×10^{19} eV with predictions for air shower simulation models for a pure proton, a pure iron and a mixed composition compatible with the FD measurements (labeled as $\langle \ln A \rangle$) [5].

The systematic uncertainties are estimated from the dispersion of the different models and compositions studied with simulated events, from variations of the quality cuts on the FD and of fitting methods applied. They are dominated by the uncertainties on the energy scale ($\sim$14%) [11].

The average values of R_μ, divided by the energy, are plotted for five energy bins in Fig. 1(left). Data points are compared to simulations for proton and iron showers, performed with QGSJETII-04 and EPOS-LHC hadronic models at $\langle \theta_{\mathrm{data}} \rangle = 67^\circ$. The predictions for protons and iron nuclei are well separated, illustrating the power of $\langle R_\mu \rangle$ as a composition estimator. The measured muon number is higher than that expected in pure iron showers, a result not in agreement with studies based on the depth of shower maximum [12] which points to an average logarithmic mass $\langle \ln A \rangle$ being between proton and iron in this energy range.

The tension between the X_{max} and R_μ measurements with respect to the expectations from different models is shown in Fig. 1 (right) which displays Auger data at 10^{19} eV compared to the predictions for different hadronic models and primary masses. The expectations for $\langle \ln R_\mu \rangle$ and $\mathrm{d}\langle \ln R_\mu \rangle / \mathrm{d} \ln E$ are compared to our measurement in Fig. 2. For QGSJETII-03, QGSJETII-04 and EPOS-LHC, $\langle \ln R_\mu \rangle$ and $\mathrm{d}\langle \ln R_\mu \rangle / \mathrm{d} \ln E$ are calculated for three different compositions: pure proton, pure iron and a composition with an average value of the logarithmic mass, $\ln A$, as obtained from the measurement of X_{max} [3]. The QGSJET01 model was not considered in that reference so that an estimate of $\ln A$ was made using the data [12] and some simple assumptions [5]. These values of $\ln A$ in turn correspond to a mean value of $\ln R_\mu$. Assuming the generalized Heitler model of hadronic air [5], it is possible to convert the estimated $\langle \ln A \rangle$ into a prediction of the logarithmic muon content which can in turn be related to $\langle R_\mu \rangle$.

When we consider the values of $\ln A$ deduced from X_{max}, the measured values of R_μ indicate that the mean number of muons in the simulations have a deficit of 30% to 80 $^{+17}_{-20}$ (sys.) % at 10^{19} eV depending on the model. The measurement of the logarithmic gain is slightly higher than the prediction but the discrepancy is smaller than for R_μ for all the models. Assuming that the logarithmic gain of real showers is well reproduced by simulations, which is supported by the fact

that the four models agree on this parameter, the measured value disfavors a pure composition hypothesis. Deviations from a constant proton (iron) composition are observed at the level of 2.2 (2.6) σ.

Different independent methods [13, 14] for vertical showers with $\theta < 60^\circ$ have been used to derive the fraction of the signal due to muons at 1000 m from the shower core with the SD array. In [13] the different features of the temporal distribution of the EM and muonic signals measured with the SD array are exploited to obtain information about the muon number. In [14] hybrid events are exploited: for each of them, a set of simulated proton and iron showers matching their longitudinal profile is produced using different hadronic interaction models. They show that the total and muonic signals are not well reproduced by the shower simulations using the most recent hadronic interaction models. Within uncertainties they are compatible with the results described above for the study of inclined showers.

3. Measurement of muon production depth

The time structure of the muon component reaching the ground can be exploited to obtain the distribution of muon production distances along the shower axis. Following a phenomenological model for muon time distributions in Extensive Air Showers (EASs) developed in [15] [16], the muon production height z of muons recorded at the ground at distance r from the core and arriving at time t can be written as

$$z \simeq \frac{1}{2}\left(\frac{r^2}{c(t-\langle t_\varepsilon\rangle)} - c(t-\langle t_\varepsilon\rangle)\right) + \Delta - \langle z_\pi\rangle \tag{3.1}$$

where $t_g \simeq t - \langle t_\varepsilon\rangle$ is the *geometric delay*, due to deviation of muon trajectories with respect to the shower axis, t_ε is the *kinematic delay*, due to the subluminal muon velocities, $\Delta = r\,\tan\theta\,\cos\xi$ is the distance from the ground impact point to the shower plane and $\langle z_\pi\rangle$ takes into account the decay length of the parent pion.

Since SD stations do not allow to measure the energy carried by each single muon, the kinematic delay cannot be directly measured and needs to be parameterized. A modeling of the muon energy distributions was then exploited to this aim [15].

By means of Eq. (3.1), a mapping between z and t at the ground is thus provided. The muon production depth (MPD) X^μ, i.e. the total amount of traversed matter in g/cm^2, is obtained integrating the atmospheric density over the range of production distances. The MPD distribution is derived adding all MPDs recorded in each of the SD stations of the event. A fit to the MPD distribution with a Gaisser-Hillas function allows us to derive the muonic shower maximum $X^\mu_{\rm max}$, i.e. the point in the shower development where the maximum number of muons is produced.

The reconstruction of the MPD distribution requires the removal of the EM contribution to the total signal. Only a residual EM contamination is contributing to the total signal at zenith angle around 60°. Since the EM signals are smaller and broader than muonic ones, a cut for $S_{\rm threshold} = 15\%$ of the maximum (peak) of the recorded signal guarantees an efficient reduction of the background and muon fractions above 85%, regardless of the energy and mass of the primary particle.

Besides, the FADC sampling frequency (40 MHz) gives rise to an uncertainty in the z reconstruction that decreases with r^2 and increases with X^μ. To keep the distortion of the reconstructed

MPD small, a cut in core distance, $r_{\rm cut}$, is thus mandatory. An optimal value $r_{\rm cut} = 1700$ m was derived from Monte Carlo simulations.

Another issue to be taken into account is that the light propagation inside the detector and the electronic response smears the muon arrival times. To compensate for this detector effect, a time offset $t_{\rm shift}$ is subtracted to each time bin. The offset value depends on $S_{\rm threshold}$: a value of 73 ns is derived from simulations.

The mean bias $[X^{\mu}_{\rm max}({\rm rec.}) - X^{\mu}_{\rm max}({\rm true})]$ stays within 10 g/cm^2, for all energies, masses and hadronic models used in simulations. The resolution, given by the standard deviation of the same distribution, ranges from 100 (80) g/cm^2 to about 50 g/cm^2 for increasing energy and proton (iron) showers. The improvement of the resolution with the energy is a direct consequence of the increase in the number of sampled muons.

The SD data of Pierre Auger Observatory between 1 January 2004 and 31 December 2012 have been used in this analysis. The selected events must satisfy the T5 trigger condition, which requires that the detector with the highest signal has all six closest neighbours operating. We considered events with zenith angle in the range $[55^\circ, 65^\circ]$ and energy greater than 20 EeV, the latter allowing the reconstruction of the MPD distribution. Furthermore, the relative uncertainty $\delta X^{\mu}_{\rm max}/X^{\mu}_{\rm max}$ must be small enough to guarantee the accuracy in the estimation of $X^{\mu}_{\rm max}$. Monte Carlo studies show that the chosen cuts introduce a negligible composition bias, smaller than 2 g/cm^2. 481 events out of 500 meet the required quality cuts.

The total systematic uncertainty on $X^{\mu}_{\rm max}$ amounts to $\approx$17 g/cm^2, which corresponds to about 25% of the proton-iron separation. The most relevant contributions come from reconstruction, differences in the hadronic interaction models, unknown primary mass and seasonal effects. A systematic underestimation by $\approx$4.5 g/cm^2 in the $X^{\mu}_{\rm max}$ determination has been found due to random accidental signals and has been corrected for.

Finally, we discovered that our simulations introduced an underestimation of the muon delay with respect to the arrival time of the shower front [17]. The effect is due to the resampling procedure, which is needed to be applied to showers simulated with a thinning method [18]. The latter is mandatory in the EASs simulations, since full simulations require large amounts of CPU time

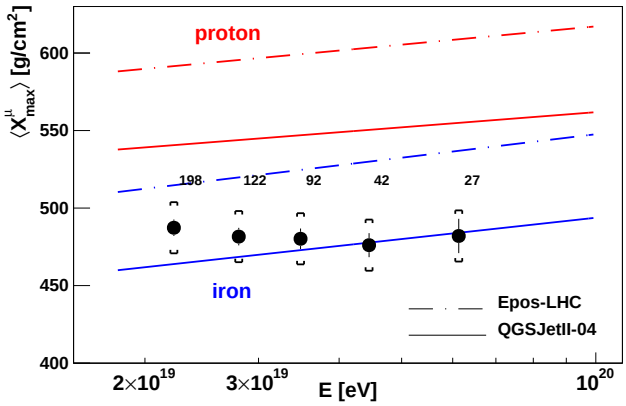

Figure 3: Evolution of $X^{\mu}_{\rm max}$ with energy. The number of events is indicated in each energy bin. Brackets represent the systematic uncertainty [17].

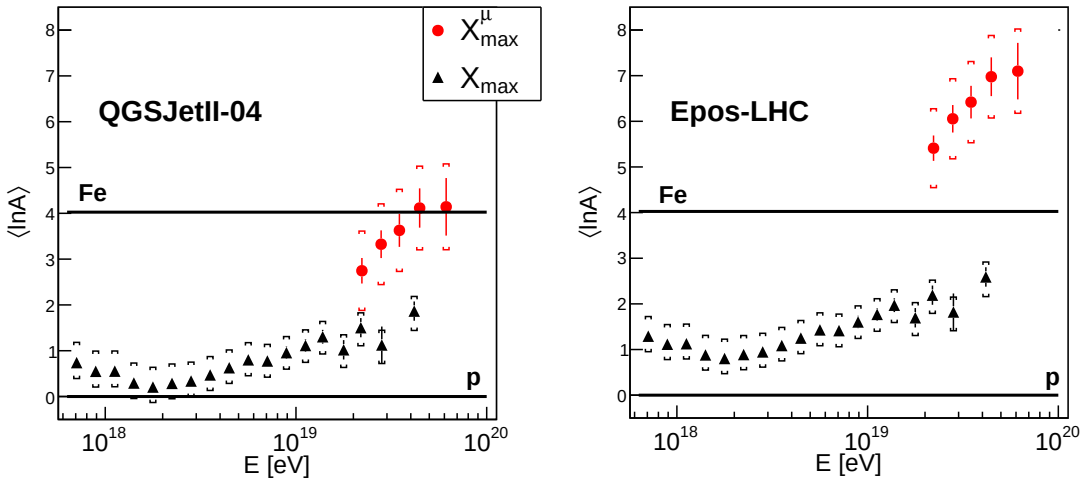

Figure 4: $\langle \ln A \rangle$ from $\langle X_{\rm max} \rangle$ (triangles) [3] and $\langle X^{\mu}_{\rm max} \rangle$ (circles) [17] vs. energy. QGSJETII-04 (left) and EPOS-LHC (right) are used as reference models. Brackets correspond to the systematic uncertainties.

and disk space. A procedure to undo the thinning is thus necessary to have a fair representation of the signals collected by the water-Cherenkov detectors. The strategy consists in the estimation of the local distribution of particles at the position of the detectors by averages over extended areas around this position. We found that the value chosen for the sampling area was not optimal and introduced an underestimation of the muon delay. While in [6] the bias due to the resampling procedure was assumed to be negligible, recent simulation studies have shown that this effect is significant, making the total bias on $X^{\mu}_{\rm max}$ reconstruction 24 g/cm^2. This bias is corrected for in simulations in order to obtain an unbiased analysis. However this correction has to be accounted for in the data (i.e. all measured $X^{\mu}_{\rm max}$ values must be reduced by an amount equal to the estimated bias).

The evolution of the measured $X^{\mu}_{\rm max}$ with energy is shown in Fig. 3. Data are grouped in five energy bins of width 0.1 in $\log_{10}(E/{\rm eV})$, except for the last bin, which contains all events with energy above $\log_{10}(E/{\rm eV}) = 19.7$ ($E = 50\,{\rm EeV}$). The interpretation of data in terms of mass composition requires a comparison with air shower simulations. As shown in Fig. 3, the two models predict a similar evolution of $X^{\mu}_{\rm max}$ for proton and iron but a considerable difference in its absolute value. While Auger data are bracketed by QGSJETII-04, they fall below the EPOS-LHC prediction for iron, thus demonstrating the power of the MPD analysis to constrain hadronic interaction models [19].

$X_{\rm max}$ and $X^{\mu}_{\rm max}$ are both correlated with the primary mass [20, 21]. Both observables can thus be converted into $\langle \ln A \rangle$ using the same interaction model.

The results of this conversion for two different hadronic models are shown in Fig. 4. With QGSJETII-04, we obtain compatible values for $\ln A$ within $1.5\,\sigma$, while in the case of EPOS-LHC the results from $\langle X^{\mu}_{\rm max} \rangle$ indicate primaries heavier than iron and the measurements are incompatible at a level of at least $6\,\sigma$. It should be noted however that QGSJETII-04 has problems to describe in a consistent way the first two moments of the $\ln A$ distribution obtained from the $X_{\rm max}$ values measured with the FD [3].

4. Conclusions

Two different analyses of the muon component have been described. By measuring the total muon content of UHE inclined showers, we observe a muon deficit in the simulations. Our data strongly disfavor light composition at 10^{19} eV.

The arrival time of muons at the ground was used to reconstruct the muon production depth distribution on an event-by-event basis. This analysis has established a new approach to study the longitudinal development of the hadronic component of EASs. The current level of systematic uncertainties does not allow to draw conclusions on composition. However, the described measurements, in correlation with the information from the EM shower profile, set valuable constraints on the most recent LHC-tuned interaction models, QGSJETII-04 and EPOS-LHC. In particular, we found that none of the interaction models provides a consistent description of both the electromagnetic and muonic shower profiles as measured by the Pierre Auger Observatory.

References

[1] I. Valiño, for the Pierre Auger Collaboration, Proc. 34th ICRC (id=271), Den Haag, Netherlands (2015).
[2] The Pierre Auger Collaboration, *Astropart. Phys.* **34** (2010) 314–326, [arXiv:1009.1855].
[3] The Pierre Auger Collaboration, *Phys. Rev.* D **90** (2014) 122005, [arXiv:1409.4809].
[4] The Pierre Auger Collaboration, accepted for publication in *Nucl. Instrum. Meth.* A (2015), [arXiv:1502.01323].
[5] The Pierre Auger Collaboration, *Phys. Rev.* D **91** (2015) 032003, [arXiv:1408.1421].
[6] The Pierre Auger Collaboration, *Phys. Rev.* D **90** (2014) 012012, [arXiv:1407.5919].
[7] The Pierre Auger Collaboration, *JCAP* (2014), [arXiv:1407.3214].
[8] M. Ave, R.A. Vazquez, E. Zas, J.A. Hinton, and A.A. Watson, *Astropart. Phys.* **14** (2000) 109, [arXiv:astro-ph/0003011].
[9] M. Ave *et al.*, *Astropart. Phys.* **14** (2000) 91–107, [arXiv:0011490].
[10] H.P. Dembinski *et al.*, *Astropart. Phys.* **34** (2010) 128–138, [arXiv:0904.2372].
[11] V. Verzi, for the Pierre Auger Collaboration, Proc. 33rd ICRC, Rio de Janeiro, Brazil (2013), [arXiv:1307.5059].
[12] A. Letessier-Selvon, for the Pierre Auger Collaboration, Proc. 33rd ICRC, Rio de Janeiro, Brazil (2013), [arXiv:1310.4620].
[13] B. Kégl, for the Pierre Auger Collaboration, Proc. 33rd ICRC, Rio de Janeiro, Brazil (2013), [arXiv:1307.5059].
[14] G.R. Farrar, for the Pierre Auger Collaboration, Proc. 33rd ICRC, Rio de Janeiro, Brazil (2013), [arXiv:1307.5059].
[15] L. Cazon, R.A. Vazquez, A.A. Watson, and E. Zas, *Astropart. Phys.* **21** (2004) 71, [arXiv:0412338].
[16] L. Cazon, R. Conceição, M. Pimenta, and E. Santos, *Astropart. Phys.* **36** (2012) 211, [arXiv:1201.5294].
[17] The Pierre Auger Collaboration, Erratum: *Phys. Rev.* D **92**, 019903 (2015)
[18] P. Billoir, *Astropart. Phys.* **30** (2008) 270.
[19] T. Pierog, B. Guiot and K. Werner, Proc. 34th ICRC (id=337), Den Haag, Netherlands (2015).
[20] The Pierre Auger Collaboration, *JCAP* **02** (2013) 026, [arXiv:1301.6637].
[21] S. Andringa, L. Cazon, R. Conceição, and M. Pimenta, *Astropart. Phys.* **35** (2012) 821, [arXiv:1301.0507].